Excitation energy and temperature-dependent Raman study of Rb_3C_{60} films

M.K. Kelly
Max-Planck-Institut für Festkörperforschung, Heisenbergstrasse 1, D-70569 Stuttgart, Germany

C. Thomsen
Institut fur Festkörperphysik, PN 5-4, Technische Universität Berlin, Hardenbergstrasse 36, D-10623 Berlin, Germany
(Received 5 July 1994)

We report Raman spectroscopy studies for Rb_3C_{60} films, which have been grown and measured, *in situ*, in an ultrahigh-vacuum chamber. We find interesting dependences of some of the vibrational modes on the excitation energy, and compare this with the corresponding optical transitions as measured by spectroscopic ellipsometry. Modes that show a strong interference with continuum excitations are enhanced for excitations corresponding to transitions involving the partially filled metallic band. Raman detection of external intermolecular modes are reported for both pure C_{60} and for Rb_3C_{60}. Some temperature dependence of these modes is observed, but no clear anomaly at the superconducting critical temperature could be determined.

I. INTRODUCTION

The vibrational properties of the alkali-C_{60} compounds such as Rb_3C_{60}, and their differences from those of pure C_{60}, are interesting for several reasons. The most obvious is the role of these vibrations for superconductivity. Since these compounds have strong ionic bonding, they also permit study of the influence of charge transfer on the molecular structure and dynamics. Since this bonding is substantially stronger than that between molecules in solid C_{60} with the same crystal symmetry, these materials also provide a means of enhancing the crystal field effects of the crystal with respect to the icosahedral symmetry of the molecule. In addition, the partial occupation of the lowest unoccupied molecular orbital in these compounds results in different optical properties than for solid C_{60}, particularly by adding transitions from this orbital level and changing transitions to this level; this can result in different excitation energy dependence for Raman spectra.

Initial Raman studies of these compounds revealed a clear signature of charge transfer to the C_{60} molecules in the form of a strong shift of one of the molecular vibrational modes.[1–3] This line could thus be used to support the finding that particular stoichiometric phases are formed. Changes in the intensities and widths of other lines also result from the reaction with Rb or K, and some modes develop asymmetric shapes that have been described with Fano line shapes.[4–7] A difference in relative intensities has been reported for infrared excitation.[7] Only weak temperature dependence has been reported for the intramolecular modes, without apparent anomalies at T_c.[8] Only recently have modes external to the molecules been reported from Raman measurements.[9] It remains to look for temperature dependence in these modes. The excitation-energy dependence of the spectra also requires further attention, particularly with reference to the changes in optical transitions associated with forming the metallic compounds.

We present here studies of the dependence on temperature, relative polarization, and excitation wavelength for light scattering on films that we have deposited and measured in ultrahigh vacuum. The wavelength dependence of the Raman cross section is compared to the dielectric function obtained from ellipsometric measurements. In particular, we see that several of the modes, including those that show a strong Fano-type interference line shape, are enhanced for excitation with red light, which probably corresponds to resonance with transitions involving the partially filled metallic t_{1u} band. We see clearly, particularly at this wavelength, low-energy modes corresponding to translation of the Rb atoms and to molecular librations. The latter in particular shows strong temperature dependence, although we are unable to discern anomalous behavior associated with the superconducting transition. Intermolecular modes were also measured for the pure C_{60} films. We analyze the line shape and symmetry of several of the modes and find at least one case where the splitting due to the crystal symmetry results in a strong change in the polarization selection rules.

II. EXPERIMENT

Because the alkali cations are quickly oxidized in air, special environment control is required for Rb_3C_{60}. In other Raman studies, the material has been reacted in and measured through a sealed container,[2] or deposited films have been made and transferred to a measurement vessel through vacuum[9] or a glovebox environment.[8] For our studies, we have grown the films, *in situ*, on the cold finger of the ultrahigh-vacuum cryostat used for our optical measurements. (For recent work on the production and purification of the material we have used for film growth, see Ref. 27.) In addition to minimizing the possibility of contamination in this way, this method allowed optical measurements during the Rb doping pro-

cess. Eliminating the need for transferring the sample also simplifies making electrical contacts to the sample and we have monitored resistance during our experiments and observed the superconducting transition.

The films were grown and measured in a turbo-pumped chamber which was baked out to reach about 5×10^{-9} Torr. Chromatographically separated C_{60} was sublimated from a Ta boat after about 10 h of outgassing slightly under the temperature used during deposition. Rubidium was evaporated from an SAES Getters alkali metal source, also after thorough outgassing. Films were grown both on Si and sapphire substrates. Four parallel gold strips were previously deposited on the sapphire substrate to enable a four-contact resistance measurement.

Films of C_{60} were first deposited on the room temperature substrate to a thickness of about 100 nm in 30 min. The film was then doped, also at room temperature, by exposure to the Rb source heated with 5.5 A. This process also required about 30 min to reach a Rb_3C_{60} stoichiometry. As discussed in more detail below, this initially also resulted in the presence of C_{60} and Rb_6C_{60} phases, as determined by the Raman measurements, presumably due to vertical inhomogeneity from limited Rb diffusion rate. These extra peaks reduced quickly in intensity within the first 1–2 h at room temperature. At our Rb exposure rate, the resistance measurement gave a quite accurate indication of the desired stoichiometry based on reaching a minimum. Additional Rb exposure, after allowing more time for Rb diffusion, did not result in appreciable further resistance decrease.

The room temperature resistivity so obtained (7–10 mΩ cm) agree with published values within the rough accuracy of our film thickness estimates.[8,10] For the as-grown films, the resistivity was approximately constant as a function of temperature down to about 50 K and then increased by about 30% with further cooling to 20 K, apparently indicating nonmetallic behavior due to grain boundaries.

In order to heat the film for annealing, with minimum outgassing of other parts, current was passed directly through the film between the two outer contacts. The process could be monitored by simultaneous measurement of the applied voltage to determine resistance. The resistance initially increased with increasing temperature and then eventually decreased slowly at stable temperature. The actual annealing temperature could not be determined since the thermocouple was not in direct contact with the film, but the thermocouple reading was above 100 °C.

After annealing, the room temperature resistance was only slightly reduced. However, it decreased nearly linearly with decreasing temperature to about 60% of the room temperature value at about 50 K, then increased slightly with cooling to T_c. The resistance then dropped to about half this value by cooling a further 8 K to our lowest temperature, 20 K. This residual resistance is presumably still due to grain boundaries or other defects and might be further improved with more complete annealing.

Resistance was measured with an ac-resistance bridge. Cooling was achieved with liquid He flow. The Raman measurements were made with a Dilor XY triple spectrometer and a charge-coupled device detector using Ar and Kr gas lasers at 458, 514, 568, and 647 nm. The laser was focused on the sample through the vacuum chamber pyrex window with a 10 cm focal length achromat lens, producing a spot size of 50–100 μm. The same $f/3.1$ lens was used for scattered-light collection. During the temperature-dependent measurements, low laser intensities of 0.25–0.5 mW were used to minimize heating. At the lowest temperature, we have compared adjustments for Bose-Einstein statistics for different power levels to determine that the 0.25 mW 647 nm excitation probably results in about 3°K heating. For the measurements on the sapphire substrate, it was necessary to avoid the signal from the substrate and its holder, since the films were not thick enough to be opaque. Therefore the measurements were made on spots over the gold strips. We also use results of ellipsometric measurements performed on similarly prepared films in the same cryostat. We have described this measurement earlier.[11]

III. C_{60} FILMS AND Rb DOPING

Before doping with Rb, we did some characterization of the pure C_{60} films using 514 nm excitation. The intramolecular modes have already received considerable study with Raman spectroscopy and our results are in good agreement;[12–14] in particular, we see the same structure as seen in the detail spectra of Ref. 14 and consistent with the fit parameters of Ref. 13. Using the triple monochromator in subtraction geometry, we have also been able to obtain clear spectra of librational modes for the low-temperature ordered phase, for which we are aware of only one report of comparable quality, obtained with infrared excitation.[15]

In Fig. 1 we show a spectrum obtained at 40 K which has been corrected for the Bose-Einstein statistical factor. We see two distinct modes at 23.4 cm^{-1} and 33.3 cm^{-1} as well as a possible broader structure near 43 cm^{-1}. The feature at 23.4 cm^{-1} has a peak height of about 10% that of the peak at 265 cm^{-1}. The mode near 33.3 cm^{-1} may be more strongly suppressed in crossed polarization than the 23.4 cm^{-1} mode. The two lines look very similar to the most prominent lines reported in Ref. 15, but correspond in energy to some of the weaker structures there. The reason we do not see the stronger peaks at lower energy is not yet clear. Since there could be five librational modes in Raman measurements,[16] it may be that we are seeing different modes due to different excitation energies. Their measurements were made with 790 nm light and showed less clearly resolved lines at higher energy. Alternately, there may be a difference due to the order between our presumed microcrystalline films and the single crystal sample of that report. We have observed a significantly higher optical density for a single crystal sample compared to the room temperature deposited films with ellipsometry measurements,[11] in agreement with other measurements.[17]

We briefly address photoinduced changes to the films. The largely accepted model is that excitation by light

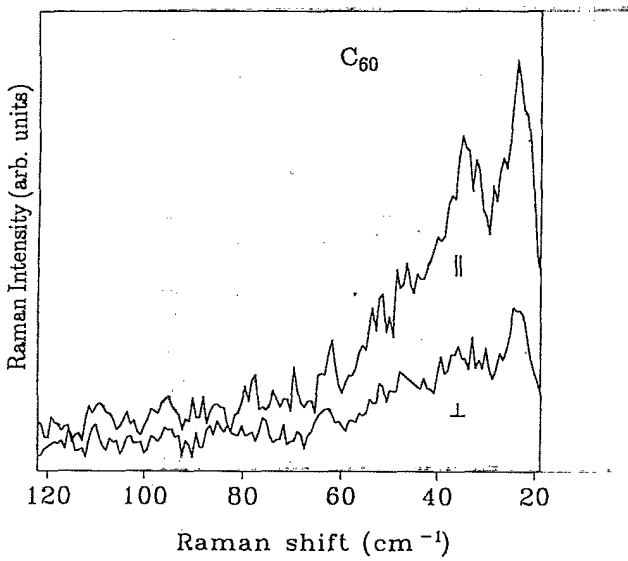

FIG. 1. Raman spectra of librational modes for pure C_{60} films at 40 K taken with detected light polarized parallel and perpendicular to the 514 nm excitation. The spectra have been corrected for Bose-Einstein statistics.

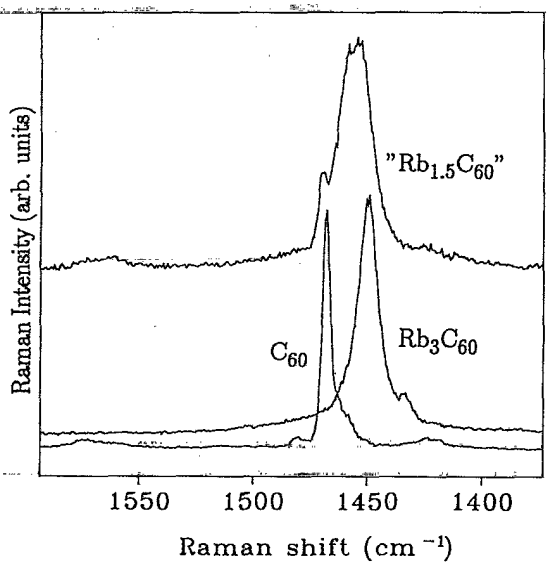

FIG. 2. Comparison of the charge-state-sensitive pinch mode for different Rb concentrations. Spectra were taken within 30 min after Rb evaporation, for excitation with 514 nm light. Relative scales are arbitrary.

above the absorption gap in these materials can cause chemical bonding between the molecules, apparently by way of an intermediate triplet excitation state.[18,19] This process results in a marked change in some of the Raman lines, particularly the strong line at 1469 cm^{-1}. Since this process is inhibited by the presence of oxygen, the explanation of these changes has been complicated with the issue of sample purity. Since our sample preparation in vacuum should be free of atmospheric contamination beyond the level of a glovebox, it is worthwhile to mention that we observe behavior consistent with the above mentioned model.

At room temperature, the films changed quickly under laser exposure so the spectra had to be taken quickly and with low power. These changes, like the shifting of the 1469 cm^{-1} peak to 1458 cm^{-1}, have been well documented. Also as previously observed, the films become stable against this change at temperatures below the ordering transition at 255 K.[20] We also observed that exposure to trace amounts of Rb, like air, seems to inhibit the photoreaction. This suggests that the role of inhibitor can be played by several types of contaminants. The effect of small amounts of Rb may result from carriers introduced into the t_{1u} band that, perhaps, contribute to the decay of the triplet state. This could also explain the stability of thin films in contact with metallic substrates which have been measured with a surface enhanced intensity.[5,21]

The development of the 1469 cm^{-1} peak with doping is shown for approximate compositions of $Rb_{1.5}$:C_{60} and Rb_3:C_{60} in Fig. 2. Raman spectroscopy has been one of the tools used to show the separation into phases of distinct stoichiometry rather than a continuous range of composition, according to the shifting of the 1469 cm^{-1} mode to distinct positions corresponding to the phases. Our spectrum corresponding to $Rb_{1.5}$:C_{60}, however, shows a broad structure between the peak at 1469 cm^{-1} for C_{60} and the corresponding position for Rb_3C_{60} at 1449 cm^{-1}.[2] From fits to our data, it appears that this structure cannot be explained as only due to a peak at 1458 cm^{-1} due to the photoreacted material. Possibly this indicates an incomplete phase separation due to relatively slow Rb diffusion at room temperature, since the spectra was taken within 30 min after the Rb exposure. As noted above, the Rb_6C_{60}, whose presence is indicated by the peak at 1433 cm^{-1} in the lower spectrum, disappears with time, apparently due to further Rb diffusion. The sample may thus not yet be in equilibrium. We note, however, that most of the peaks for intermediate stoichiometry are consistent with having a mixture of Rb_3C_{60} and C_{60}. We suggest another possible cause for the broadening of the $A_g(2)$ peak.

This peak has been observed to shift, not only due to doping with alkali metals, but more generally to changes in charge state. More particularly, it has been shown that contact of very thin films with metallic substrates causes this line to shift, apparently due to charge transfer from the metal to the high electron affinity molecules.[5,21] Such a transfer could also take place between metallic Rb_3C_{60} grains and pure C_{60} grains in a mixed film. For a very fine grain structure, which might be expected here, the surface of these grains will be a large part of the solid. Since this charge transfer will decrease away from the grain surface, a significant inhomogeneous broadening could be expected, as in our spectra. This effect might also be expected in other charge sensitive measurements, such as in photoemission spectra for intermediate doping.

IV. Rb_3C_{60}: EXCITATION ENERGY DEPENDENCE

The spectra of the intramolecular vibrational modes for four excitation energies are shown in Fig. 3. These are similar to earlier results,[2–8] most of which were made

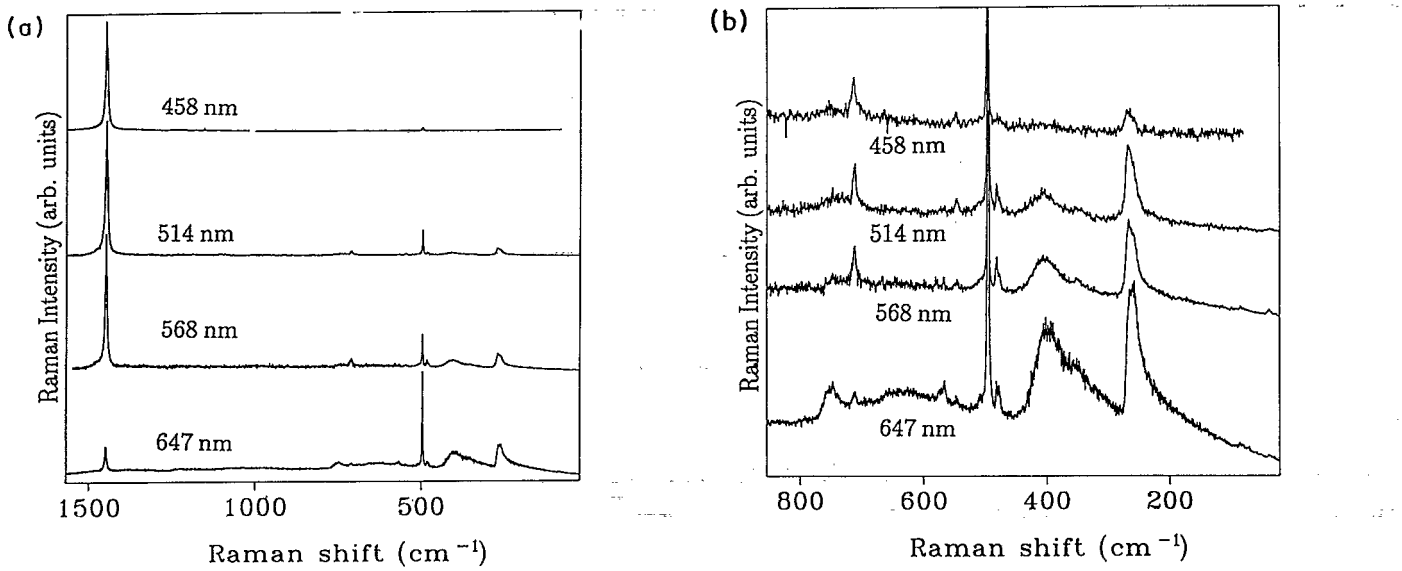

FIG. 3. (a) Comparison of the Raman spectra of Rb_3C_{60} for several excitation energies. All measurements are from room temperature for detected light polarized parallel to the excitation. Correction has been made for Bose-Einstein statistics. Relative scales have been adjusted for visibility. Intensities are compared in the text and Table I. (b) same as (a) but with expanded scale.

at 514 nm or 488 nm. We concentrate here on details revealed through comparison of the results using different laser lines. The spectrum from the 647 nm laser shows the most interesting differences.

In Table I we summarize the results of fitting the most prominent peaks with fundamental line shapes. Most of the fits use a convolution of Gaussian and Lorentzian forms which allows for both lifetime and instrumental broadening. Fano line shapes, $A(q+\epsilon)^2/(1+\epsilon^2)$ with $\epsilon = (E-E_0)/\Gamma$, which model interference between the lines and a continuum, have also been used in some cases. Intensities are compared using the areas under the peaks

TABLE I. Excitation-energy dependence of Raman intensity normalized to the intensity of the corresponding 712 cm^{-1} line. Intensities correspond for Lorentzian fits (L) to peak area, and for Fano fits (F) to Aq^2 as described in the text. Polarization ratios $I_\perp/I_\parallel$ are given in square brackets.

		Normalized Raman intensity (I/I_{712}) [polarization ratio]			
		647 nm	568 nm	514 nm	458 nm
$A_g(1)$					
495.5 cm^{-1}	(L)	10 [.03]	3.1	3 [0.05]	3
481 cm^{-1}	(L)	0.3 [0.0]	0.6	0.15 [0.0]	0.1
477 cm^{-1}	(L)	0.5 [0.5]	0.3	0.15 [0.5]	0.1
$A_g(2)$					
1449 cm^{-1}	(L)	13 [.03]	40	40 [0.01]	50
$H_g(1)$					
267 cm^{-1}	(L)	8 [0.65]	2.1	2 [0.5]	2
261 cm^{-1}	(F)	0.4 [0.65]	0.25	0.1 [0.6]	0.06
		$q=-1.5$	$q=-4.4$	$q=-5$	$q=100$
$H_g(2)$					
415 cm^{-1}	(F)	0.35 [0.65]	0.16	0.05 [0.5]	0.04
		$q=-1.7$	$q=-4.1$	$q=-5$	$q=-18$
$H_g(3)$					
712 cm^{-1}	(L)	1 [0.07]	1	1	1
$H_g(4)$					
750 cm^{-1}		>1	<1	<1	<1

for Lorentzian line shapes and using a peak height measure Aq^2 for the Fano line shapes. After normalizing to laser power and detector sensitivity, the sharp line at 712 cm^{-1} is found to be most nearly constant with excitation energy (within a factor of about 2), so the final normalized intensities are given as a ratio with respect to the corresponding 712 cm^{-1} line.

In general, we observe that the lower energy modes are enhanced for excitation with red light, particularly those near 270, 415, 496, and 750 cm^{-1}, as well as the lower energy intermolecular modes which we will discuss in the next section. This is similar to the infrared-excitation results of Ref. 7. In addition, a broad structure is seen around 635 cm^{-1} for red excitation, which may be either a continuum excitation or a luminescence effect. The higher energy modes, of which only the $A_g(2)$ mode at 1449 cm^{-1} is very distinct, are enhanced for higher exciting photon energy. The spectra for the blue 458 nm laser is, however, distorted by the strong wavelength dependence of the detector sensitivity at this wavelength. This effect should be responsible for much of the intensity increase in the background above 1000 cm^{-1}.

In order to explain the dependence on excitation wavelength, we consider the optical properties of Rb_3C_{60} and pure single-crystal C_{60} as obtained by ellipsometry, as shown in Fig. 4. The latter results are very similar to earlier results from films containing a small fraction of C_{70} as well.[11] The main difference is a weak feature near 3.1 eV resulting from the C_{70}. There is also an increased optical density of about 25% for the crystal relative to the films grown at room temperature. The composition

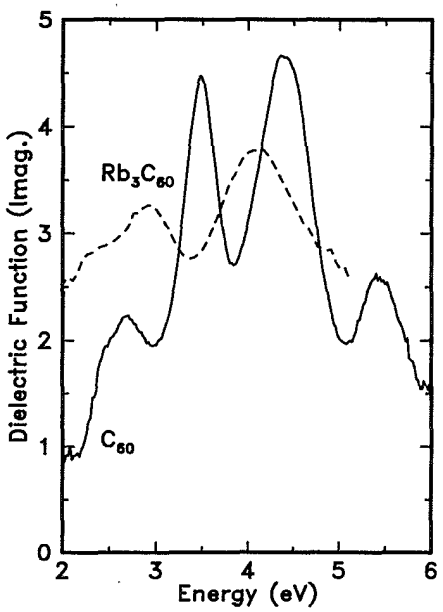

FIG. 4. Optical transitions of C_{60} and Rb_3C_{60} represented by the imaginary part of the dielectric function, obtained from room temperature ellipsometric measurements of single-crystal C_{60} and Rb_3C_{60} films prepared similarly to those of the Raman measurements. The absolute value of the latter may be somewhat influenced by possible film inhomogeneity and the vacuum chamber windows.

of the Rb_3C_{60} film used for this measurement was not as well characterized and may be somewhat inhomogeneous with some Rb_6C_{60} present, but the general spectral changes are consistent with other studies.[22,23] The absolute magnitude of this spectrum may also be somewhat influenced by the windows of the vacuum chamber.

As discussed in Ref. 11, the double structure at 2.4–2.6 eV corresponds to the first allowed interband transition with $h_u \rightarrow t_{1g}$ molecular character, transitions from the highest occupied to the second lowest unoccupied orbital. The edge near 1.9 eV corresponds to forbidden $h_u \rightarrow t_{1u}$ transitions, i.e., to the lowest unoccupied orbital band. With half-occupation of the t_{1u} band from the Rb electrons, transitions from this band should become possible to the next t_{1g} and h_g levels, and transitions to this band should be weakened. Using the energy diagram of Ref. 11 the new transitions would be expected near 1 eV and 2.6 eV while the 3.5 eV feature should decrease. This agrees reasonably with Fig. 4 and with electron-energy-loss spectroscopy[22] and absorption measurements,[23] although the higher energy induced peak appears to be closer to 2.9 eV.

In addition to these changes expected on the basis of a rigid band filling model, Fig. 4 also shows an increase in absorption near 2 eV. Unless some band spacings are significantly shifted from the pure C_{60}, this should correspond to increased oscillator strength for the $h_u \rightarrow t_{1u}$ transition, and thus involves the metallic band of the compound.

It is thus likely that the modes which are enhanced for red excitation are in resonance with transitions to the metallic band. We used the blue laser line to see if a similar result would be seen for the transition $t_{1u} \rightarrow h_g$ between 2.6 and 3.0 eV. Within the limitations of our weak detector sensitivity in this region, however, there does not appear to be a significant difference compared to excitation at 514 nm. Possibly the 467 nm is still not high enough energy to access this transition. Enhancement of the same modes has been seen with infrared excitation which could correspond to the $t_{1u} \rightarrow t_{1g}$ transition from the metallic band.[7] The enhancement of the 1448 cm^{-1} line with higher excitation energy may be due to specific resonance with the $h_u \rightarrow t_{1g}$ transitions which appear to dominate this energy range. This mode is also enhanced for measurements on pure C_{60} at energies corresponding to the absorption peaks in Fig. 4.[13,24]

V. Rb_3C_{60}: INTERNAL MODES

The two broad structures near 270 cm^{-1} and 415 cm^{-1} correspond to the $H_g(1)$ (squashing mode) and $H_g(2)$ modes of the molecule. They are both strongly enhanced for red excitation. This enhancement has already been seen for excitation in the infrared at 1.06 μm.[7] Both modes also show significant broadening and have been analyzed as Fano line shapes.[4,7,8] We have been able to observe additional detail in these structures.

The 270 cm^{-1} mode is found to be too steep on the high-energy side relative to the low-energy side for a single Fano line and shows a double peak. We have ob-

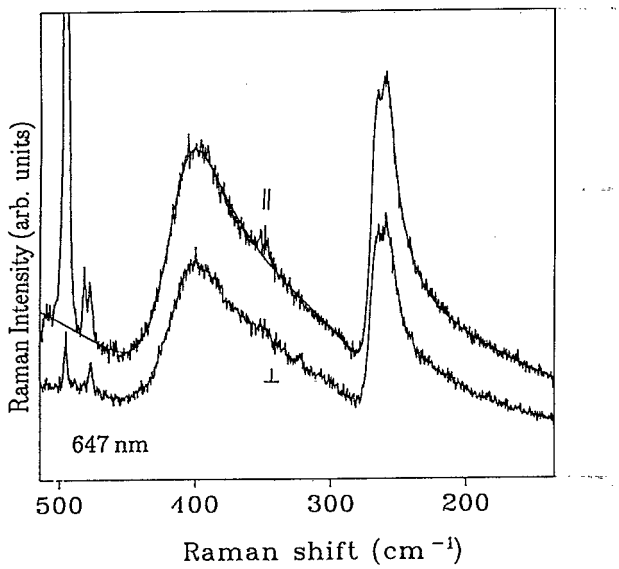

FIG. 5. Raman spectra of Rb_3C_{60} with 647 nm excitation at room temperature for parallel and crossed polarization. Lines at 496, 481, and 350 cm^{-1} are strongly polarized. A fit of the interference broadened features including a Lorentzian at 267 cm^{-1} is also shown. The spectra are shown at the same scale and have been corrected for Bose-Einstein statistics.

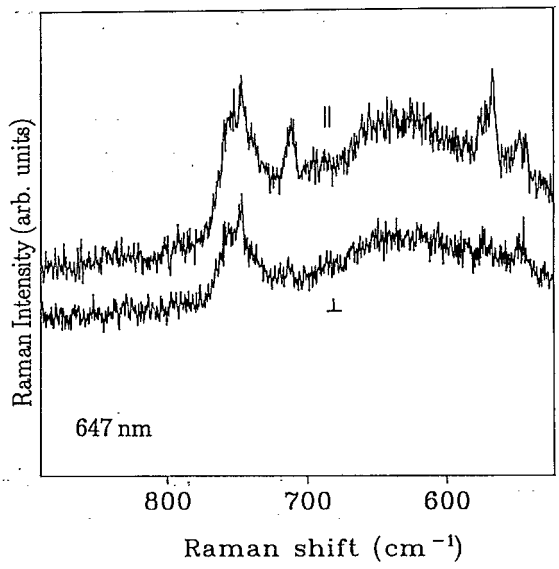

FIG. 6. Raman spectra of Rb_3C_{60} with 647 nm excitation at room temperature for parallel and crossed polarization. Lines at 712 and near 550 cm^{-1} are strongly polarized. The spectra are shown at the same scale.

tained a very good fit using a Fano line shape and a Lorenzian at slightly higher energy, as shown in Table I and in Fig. 5. This mode was resolved into three lines for the low-temperature phases of C_{60},[14] so the splitting is also not surprising in this case. It would be interesting to understand the symmetry of the splitting which causes only part of this mode to interfere with a continuum. Both line shapes have a polarization ratio of about 0.65, as does the broader structure at 415 cm^{-1}. For both modes, the interference parameter q and the continuum intensity parameter A are greater for excitation with red light, suggesting that the continuum excitations are related to the metallic band. These fits were made allowing a linear background as well. This background became negative at low energies, which probably indicates that the continuum intensity should actually decrease for low Raman shift. This would correspond in part to an energy-dependent parameter A.

The 415 cm^{-1} feature shows even stronger coupling to this continuum, and is significantly shifted from the molecular $H_g(2)$ modes near 430 cm^{-1}. Additional structure is seen near 350 and perhaps 290 cm^{-1}. These structures may be related to weak peaks observed in the low-temperature C_{60} spectra,[6] and presumably due to other vibrational modes which are only detected due to symmetry reduction in the solid. Note that the feature at 350 cm^{-1} is more strongly polarized.

As previously reported, the $A_g(1)$ line is even narrower in this metallic compound than for the pure molecular solid, and remains completely polarized.[8] Of the two smaller peaks at 481 and 478 cm^{-1}, the first is completely polarized and the latter has a polarization ratio of about 50%.

In the red excitation spectrum a broad background peak near 635 cm^{-1} is observed. In general, all lines below this peak seem to be enhanced at this wavelength. The weak features near 520 and 550 cm^{-1} (Fig. 6) also seem to have some Fano line-shape character. Possibly this background structure represents the continuum excitations with which all these lines interfere. At higher energy excitation there is also background intensity, but with less clear structure. As observed at 514 nm, the background above 1000 cm^{-1} which increases for higher Raman shift seems to have increased with time or in one case after a pump shutdown resulted in a pressure increase. Thus there may be a contribution due to luminescence of some contamination species. As mentioned before, the large intensity increase for high Raman shift for the 467 nm spectrum is also due to the rapid increase in spectrometer response at longer wavelengths.

While the sharp line at 712 cm^{-1} has similar intensity for all wavelengths, the more complex structure near 750 cm^{-1} is again enhanced for red light, while it only shows a weak shoulder for shorter wavelengths. The first, which should correspond to the $H_g(3)$, mode apparently shows strong crystal field splitting, which can be expected to separate it into E_g and F_g components. The former would have complete parallel polarization response. As was seen in the Rb_6C_{60} composition, we observe complete polarization for the 712 cm^{-1} peak,[12] as well as for the feature near 550 cm^{-1}. The $H_g(4)$ feature at 750 cm^{-1} seems to contain several peaks, but they all show similar polarization character.

The higher energy H_g modes are not very distinct in this metallic compound. The two broad structures near 1100 and 1250 cm^{-1}, which are most distinct with the green or blue light, are probably due to the $H_g(5)$ and $H_g(6)$ modes. These modes also seem to show strong

splitting for C_{60}, especially at low temperatures.[14] The $H_g(7)$ and $H_g(8)$ which are near 1425 and 1570 cm^{-1} in the molecular solid may be broadened into the wings around the strong 1449 cm^{-1} peak here. This latter peak also remains fully polarized in the compound, and at least in our samples is rather broader than in C_{60}.

VI. Rb_3C_{60}: EXTERNAL MODES

We have also observed modes at lower Raman shift corresponding to a translational mode of the Rb atoms located in the tetrahedral sites near 80 cm^{-1} and the librational mode near 40 cm^{-1}, as shown in Fig. 7, where the spectra have been corrected for the Bose-Einstein occupation factor. The former has recently been reported for Raman measurements with 790 nm light[9] and both have been observed using inelastic neutron scattering.[25,26] The Rb translational mode is also seen to be enhanced for the red light, while the other seems to be similarly strong for red, yellow, and green light. We can also see that the large width of the translation line which was remarked upon in Ref. 9 is probably due to interference with the continuum, causing a Fano line-shape. The librational mode may also have such a line shape, but this conclusion is more tentative since the feature is close to the limit of our approach to the laser line for these samples and would be sensitive to residual scattered laser light. This librational line also appears to be strongly polarized, while the translational mode is present for both parallel and crossed polarization.

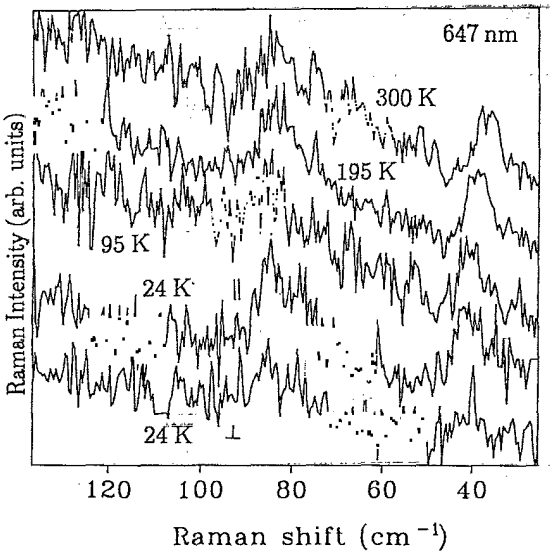

FIG. 7. Raman spectra of the intermolecular modes of Rb_3C_{60} and their temperature dependence. Measurements were made with 647 nm excitation. All spectra have been adjusted for Bose-Einstein statistics. The low-temperature spectra, for which the sample was superconducting, are shown for parallel and crossed polarization. Relative scales have been adjusted for similarity.

VII. Rb_3C_{60}: TEMPERATURE DEPENDENCE

As mentioned above, we have been able to cool to about 8 K below T_c, or about 20 K and using 0.25 mW at 647 nm appears to raise this temperature by about 3 K. We have thus investigated the temperature dependence of the observed modes, both for continuous changes and possible changes associated with the superconducting transition.

The internal molecular modes show only slight change with temperature, as has been reported elsewhere.[8] For most of the modes, our statistical uncertainty and the large width of the lines prevents determination of any changes. Both A_g modes show a slight hardening with decreasing temperature which is marginally observable with our resolution. The higher energy mode shifts by about 1 cm^{-1} between 300 and 23 K. The lower mode hardens by about 1 cm^{-1} between 300 and 35 K and then appears to shift another 0.5 cm^{-1} upward upon cooling below T_c to 23 K. This latter shift seems disproportionately large and may be related to the transition, but the effect is really on the limit of what we can resolve. Higher resolution studies could be interesting.

Such small changes are not discernable for the wider $H_g(1)$ and $H_g(2)$ structures due to their complicated shapes and a strong dependence of our fits on the assumed continuum background. We observe some change in shape of the $H_g(2)$ structure with temperature as was indicated in Ref. 7. At lower temperatures it seems to get rounder with the energy region near 350 cm^{-1} gaining in relative intensity. Possibly this is even due to the separate structure near this energy. However, it seems that this effect is rather continuous with temperature change and not related to the superconducting transition.

Not surprisingly, the external modes show stronger temperature dependence. Most clearly, the librational mode shifts from about 38.5 cm^{-1} at 300 K to about 44 cm^{-1} near 30 K. (Note that these values correspond to E_0 from Fano line-shape fits; the peak centers are at somewhat lower energy.) On cooling to 23 K this feature may soften by 1–2 cm^{-1} but changes of this magnitude are difficult for us to separate from other line-shape changes or the details of the background. The asymmetric translational line can be fit well with a Fano line-shape and an energy position of about 85 cm^{-1} at 300 K. This energy seems to harden to about 87.5 cm^{-1} near 30 K. Cooling to 23 K seems to give a more symmetric peak and fits suggest a softening of 2–3 cm^{-1}. The change in shape makes this effect even less certain, however, and the fit is again quite dependent on background slope. Changes near T_c could be particularly interesting in this mode because of its likely proximity to the gap energy. Observation of possible gap-related effects on the spectra might be aided by reaching lower temperatures than possible in these measurements, since the gap could still be expected to increase somewhat. In addition, the finite resistance of our sample below T_c, which is probably due to resistive junctions between grains, may indicate that a higher quality sample such as a single crystal could exhibit better defined details.

VIII. CONCLUSION

In this study, we have seen that good advantage can be made of using multiple excitation energies in Raman studies of these materials. As in the pure molecular solids, these compounds also exhibit a richness in mode splittings, polarization response, and resonance behavior, much of which remains to be characterized. Our observation of the low-energy external modes indicates limits in the size of effects due to the superconducting transition, but suggests interest in higher precision measurements.

ACKNOWLEDGMENTS

Thanks are due to A. Mittelbach and W. Hönle for their work in production and purification of the material we have used for film growth, and to E. Schönherr for the single crystal we used for the ellipsometry measurements.

[1]M. G. Mitch, S. J. Chase, and J. S. Lannin, Phys. Rev. Lett. **68**, 883 (1991).
[2]S. J. Duclos, R. C. Haddon, S. Glarum, A. F. Hebard, and K. B. Lyons, Science **254**, 1625 (1991).
[3]A. Zahab, J. L. Sauvajol, L. Firlej, R. Aznar, and P. Bernier, J. Phys. I **2**, 7 (1992).
[4]Ping Zhou, Kai-An Wang, A. M. Rao, P. C. Eklund, G. Dresselhaus, and M. S. Dresselhaus, Phys. Rev. B **45**, 10 838 (1992).
[5]M. G. Mitch, S. J. Chase, and J. S. Lannin, Int. J. Mod. Phys. B **6**, 4013 (1992).
[6]M. G. Mitch, S. J. Chase, and J. S. Lannin, Phys. Rev. Lett. **68**, 883 (1992).
[7]V. N. Denisov, A. A. Zakhidov, R. Danieli, G. Ruani, R. Zamboni, C. Taliani, K. Imaeda, K. Yakushi, H. Inokuchi, and Y. Achiba, Int. J. Mod. Phys. B **6**, 4019 (1992).
[8]Ping Zhou, Kai-An Wang, P. C. Eklund, G. Dresselhaus, M. S. Dresselhaus, Phys. Rev. B **48**, 8412 (1993).
[9]M. G. Mitch and J. S. Lannin, Phys. Rev. B **48**, 16 192 (1993).
[10]R. C. Haddon *et al.*, Nature **350**, 320 (1991).
[11]M. K. Kelly, P. Etchegoin, D. Fuchs, W. Krätschmer, and K. Fostiropoulos, Phys. Rev. B **46**, 4963 (1992).
[12]G. Dresselhaus, M. S. Dresselhaus, and P. C. Eklund, Phys. Rev. B **45**, 6923 (1992).
[13]P. H. M. van Loosdrecht, P. J. M. van Bentum, M. A. Verheijen, and G. Meijer, Chem. Phys. Lett. **198**, 587 (1992).
[14]M. Matus and H. Kuzmany, Appl. Phys. A **56**, 241 (1993).
[15]P. J. Horoyski and M. L. W. Thewalt, Phys. Rev. B **48**, 11 446 (1993).
[16]W. Que and M. B. Walker, Phys. Rev. B **48**, 13 104 (1993).
[17]P. Milani, M. Manfredini, G. Guizzetti, F. Marabelli, M. Patrini, Solid State Commun. **90**, 639 (1994).
[18]Ping Zhou, A. M. Rao, Kai-An Wang, J. D. Robertson, C. Eloi, Mark S. Meier, S. L. Ren, Xiang-Xin Bi, and P. C. Eklund, Appl. Phys. Lett. **60**, 2871 (1992).
[19]A. M. Rao, Ping Zhou, Kai-An Wang, G. T. Hager, J. M. Holden, Ying Wang, W.-T. Lee, Xiang-Xin Bi, P. C. Eklund, D. S. Cornett, M. A. Duncan, and I. J. Amster, Science **259**, 955 (1993).
[20]P. H. M. van Loosdrecht, P. J. M. van Bentum, and G. Meijer, Chem. Phys. Lett. **205**, 191 (1993).
[21]Yun Zhang, Yuhua Du, J. R. Shapley, and M. J. Weaver, Chem. Phys. Lett. **205**, 508 (1993).
[22]E. Sohmen, J. Fink, and W. Krätschmer, Europhys. Lett. **17**, 51 (1992).
[23]T. Pichler, M. Matus, J. Kürti, and H. Kuzmany, Solid State Commun. **81**, 859 (1992).
[24]M. Matus, H. Kuzmany, and W. Krätschmer, Solid State Commun. **80**, 839 (1991).
[25]C. Christides, D. A. Neumann, K. Prassides, J. R. D. Copley, J. J. Rush, M. J. Rosseinsky, D. W. Murphy, and R. C. Haddon, Phys. Rev. B **46**, 12 088 (1992).
[26]B. Renker, F. Gompf, H. Schober, P. Adelmann, H. J. Bornemann, R. Heid, Z. Phys. B **92**, 451 (1993).
[27]A. Mittelbach, W. Hönle, H. G. von Schnerring, J. Carlsen, R. Janiak, and H. Quast, Angew. Chem. Int. Ed. **104**, 1640 (1992).